



HIGH-SPEED PHOTOMETRY OF THE DISINTEGRATING PLANETESIMALS AT WD1145+017: EVIDENCE FOR RAPID DYNAMICAL EVOLUTION

B. T. GÄNSICKE¹, A. AUNGWEROJWIT², T. R. MARSH¹, V. S. DHILLON^{3,4}, D. I. SAHMAN³, DIMITRI VERAS¹, J. FARIHI⁵, P. CHOTE¹,
R. ASHLEY¹, S. ARJYOTHA⁶, S. RATTANASOON⁷, S. P. LITTLEFAIR³, D. POLLACCO¹, AND M. R. BURLEIGH⁸

¹Department of Physics, University of Warwick, Coventry CV4 7AL, UK; boris.gaensicke@warwick.ac.uk

²Department of Physics, Faculty of Science, Naresuan University, Phitsanulok 65000, Thailand

³Department of Physics and Astronomy, University of Sheffield, Sheffield S3 7RH, UK

⁴Instituto de Astrofísica de Canarias, E-38205 La Laguna, Santa Cruz de Tenerife, Spain

⁵Department of Physics and Astronomy, University College London, London WC1E 6BT, UK

⁶Program of Physics, Faculty of Science and Technology, Chiang Rai Rajabhat University, Chiang Rai, 57100, Thailand

⁷National Astronomical Research Institute of Thailand, 191 Siriphanich Bldg., Huay Kaew Road, Suthep, Muang, Chiang Mai 50200, Thailand

⁸Department of Physics and Astronomy, University of Leicester, Leicester LE1 7RH, UK

Received 2015 December 30; accepted 2016 January 9; published 2016 February 3

ABSTRACT

We obtained high-speed photometry of the disintegrating planetesimals orbiting the white dwarf WD 1145+017, spanning a period of four weeks. The light curves show a dramatic evolution of the system since the first observations obtained about seven months ago. Multiple transit events are detected in every light curve, which have varying durations ($\simeq 3$ –12 minutes) and depths ($\simeq 10\%$ –60%). The time-averaged extinction is $\simeq 11\%$, much higher than at the time of the *Kepler* observations. The shortest-duration transits require that the occulting cloud of debris has a few times the size of the white dwarf, longer events are often resolved into the superposition of several individual transits. The transits evolve on timescales of days, both in shape and in depth, with most of them gradually appearing and disappearing over the course of the observing campaign. Several transits can be tracked across multiple nights, all of them recur on periods of $\simeq 4.49$ hr, indicating multiple planetary debris fragments on nearly identical orbits. Identifying the specific origin of these bodies within this planetary system, and the evolution leading to their current orbits remains a challenging problem.

Key words: minor planets, asteroids: general – planetary systems – stars: individual (WD 1145+017)

Supporting material: tar.gz file

1. INTRODUCTION

Planets around main-sequence stars are ubiquitous (Cassan et al. 2012; Fressin et al. 2013), and a significant fraction of them are predicted to survive the giant branch evolution of their host stars (Mustill & Villaver 2012; Veras et al. 2013). This expectation is corroborated by the detection of debris accreted into the photospheres of white dwarfs, resulting from the tidal disruption (Debes & Sigurdsson 2002; Jura 2003) of planetary bodies among $\simeq 25\%$ –50% of all white dwarfs (Zuckerman et al. 2003; Koester et al. 2014). Little is known so far regarding the detailed nature of the disrupted objects, the exact origin within their planetary systems, and the processes resulting in their disintegration and subsequent circularization (Debes et al. 2012; Veras et al. 2014b, 2015c) and leading to dusty debris disks with typical radii of $\simeq 1 R_{\odot}$, which have been detected as infrared excess to $\simeq 40$ white dwarfs (Rocchetto et al. 2015). The life times of these disks are thought to be long compared to human timescales, $\sim 10^4$ – 10^6 years (Girven et al. 2012), yet, a small number of disks show substantial variability on timescales of years to decades in their infrared flux (Xu & Jura 2014) or in the strength and morphology of optical emission lines from gaseous disk components (Wilson et al. 2014, 2015; Manser et al. 2016), indicative of ongoing dynamical processes.

Recently, Vanderburg et al. (2015) announced the discovery of transits in the *K2* light curve of the white dwarf WD 1145+017, recurring every $\simeq 4.5$ hr, i.e., near the Roche-limit for a strengthless rubble pile. As WD 1145+017⁹ also exhibits both a large infrared excess, as well as strong photospheric metal pollution, Vanderburg et al. (2015) interpreted the transit events as the signature of debris clouds from a disintegrating planetesimal occulting the white dwarf. Given the detection of multiple periodicities in the *K2* light curve, Vanderburg et al. (2015) argued for the presence of several, possibly six individual planetesimals. Following up WD 1145+017 with ground-based photometry, Vanderburg et al. (2015) and Croll et al. (2015) detected several relatively short ($\simeq 10$ minutes) and deep ($\simeq 40\%$) transit events that did, however, only occasionally repeat at the same phase during subsequent observations. These optical transits were compatible with the $\simeq 4.5$ hr period identified in the *K2* data. High-resolution spectroscopy obtained by Xu et al. (2016) reveals strong, broad circumstellar low-ionization absorption lines of several metals, adding further evidence to the ongoing disintegration of a planetary body or bodies.

Here we report the first high-speed photometry of the transits at WD 1145+017, which show a dramatic evolution of the system in the seven months since the observations of Vanderburg et al. (2015) and Croll et al. (2015) and suggest a rapid evolution of the planetesimals and their debris.

2. OBSERVATIONS

We obtained high-speed photometry with the frame-transfer camera ULTRASPEC (Dhillon et al. 2014) mounted on the

⁹ WD 1145+017 was first identified as a white dwarf by Berg et al. (1992) in the Large Bright Quasar Survey, and later re-discovered as part of the Hamburg-ESO survey (Friedrich et al. 2000). Adopting a white dwarf mass of $0.6 M_{\odot}$, Vanderburg et al. (2015) determined $T_{\text{eff}} = 15\,900$ K, corresponding to a cooling age of 175 Myr, and a distance of 174 pc.

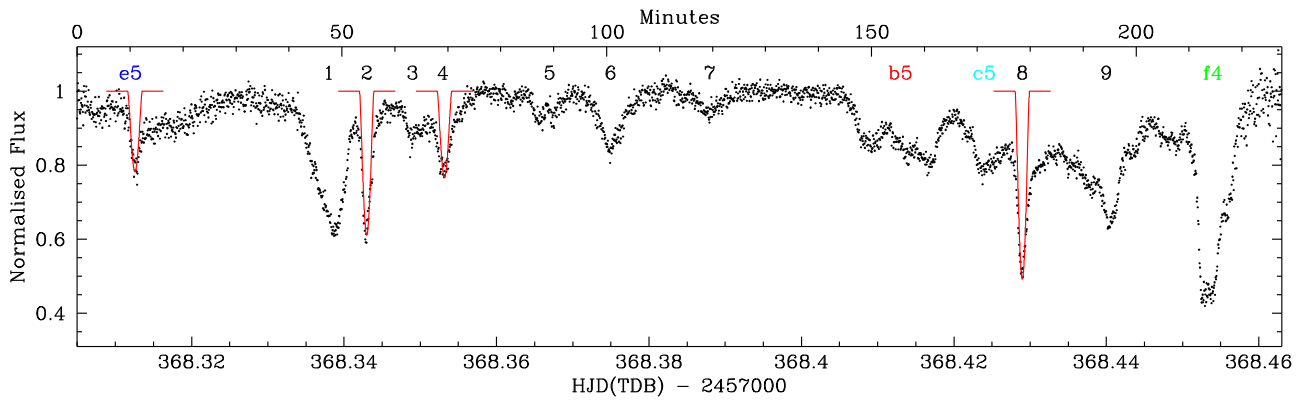


Figure 1. TNT/ULTRASPEC high-speed (5 s) photometry of WD 1145+017, obtained over 3.9 hr on 2015 December 11, illustrating the varied and complex nature of the multiple transit events. Many of the broader transits display sub-structure that appears to be the superposition of several shorter events, e.g., #4 and b5. Transits labeled in color can be tracked in phase across multiple nights (see Figure 2). Simple transit models are overlaid in red, see Section 4 for details.

2.4 m Thai National Telescope (TNT) on Doi Inthanon over eleven nights in between 2015, November 28, and December 22. We used a KG5 short-pass filter which cuts off red light beyond 7000 Å, and exposure times of three to eight seconds, with 15 ms dead time between exposures. Additional observations were obtained on 2015, December 17, 23–25, using the Warwick 1 m (W1m) telescope at the Roque de Los Muchachos Observatory on La Palma, a robotic F/7 equatorial fork-mounted telescope with a dual-beam camera system. These data were acquired in engineering mode using the reflecting arm of the instrument, which currently contains a fixed $V + R$ filter with an Andor DW936 camera (featuring a back-illuminated $2k \times 2k$ CCD with $13.5 \mu\text{m}$ pixels). The camera was operated with 2×2 binning to reduce the readout time to 3 s, giving an exposure cadence of 23 s. The combined TNT and W1m observations add up to 39.3 hr on-target, and were carried out under a variety of conditions. A full log of the observations is available. Differential photometry was computed using the nearby comparison stars SDSS J114840.49+012954.7 and SDSS J114825.30+013342.2. As we used non-standard broad-band filters in both instruments, the data were not absolutely calibrated, and we normalized all light curves to an out-of-transit flux of one. The normalized light curves will be made available through the VizieR service at CDS.

A typical TNT/ULTRASPEC light curve is shown in Figure 1. It is immediately apparent that the morphology of the transits has dramatically evolved since 2015 April/May, when the observations of Vanderburg et al. (2015) and Croll et al. (2015) were taken: The light curve is riddled with numerous transit events varying in duration from ≈ 3 to ≈ 12 minutes with depths of $\approx 10\%$ to $\approx 60\%$. Many of the transit features overlap, such that there are only short segments of the light curve which appear unattenuated by debris. The full sequence of light curves obtained during this campaign shown in Figure 2 (folded on a period of 4.4930 hr, see Section 3) illustrates that the transits undergo significant night-to-night variations, but that nevertheless individual events can be confidently identified and tracked across multiple nights.

3. TRANSIT ANALYSIS

The complex and highly variable morphology of the transit events challenges standard period searches. The strongest

signal in an Analysis-of-Variance periodogram is found at 4.498 hr, close to the period that Vanderburg et al. (2015) reported from the analysis of the *K2* data. However, phase-folding all light curves on this period washes out many of the features.

We identified distinct transit features in each light curve, and measured mid-transit times visually cross-correlating each transit profile with its mirror image with respect to time. This method has been developed initially for the analysis of eclipsing cataclysmic variables (Pyrzas et al. 2012), and has been found to be more robust in the case of asymmetric transit shapes compared to fitting an analytical function. Estimated uncertainties in the mid-transit times are 30–60 s, depending on the shape of the individual transit. We then attempted to group individual transit features that can be identified across multiple nights, beginning with the broad, irregularly shaped dip labeled b1–b8 in Figure 2. Fitting a linear ephemeris to the transit times of this feature results in $P = 4.49252(11)$ hr, where the uncertainty is purely statistical in nature. The true uncertainty in the period is likely to be larger due to the complex shape of the transit, and the associated difficulty in accurately defining the mid-transit time.

We identified five additional groups of transits that appear to be related to the same material occulting the white dwarf on at least three different nights (labeled a, c, d, e, f in Figure 2; #a1 and #a2 are the superposition of two very closely spaced short events), and linear ephemeris fits to the corresponding groups of transit times result in periods in the range 4.491–4.495 hr (Table 1), with a mean of 4.4930(13) hr. Adopting this mean period, we computed orbital phases for the six groups of transits, which are shown in Figure 3. Various other transit features can be identified in two subsequent light curves (e.g., 2015 December 10#1,2,3,4 and 2015 December 11#1,4,5,6; 2015 December 22#1–4 and 2015 December 23#2–5), which are also consistent with a 4.49 hr period. We were not able to identify a group of transit events with a significantly different period, in particular we were not able to recover the periods longer than ≈ 4.49 hr discussed by Vanderburg et al. (2015). The periods from our analysis are similar to those found by Croll et al. (2015), and are all slightly, but significantly, shorter than the 4.4988h period derived from the *K2* data (Vanderburg et al. 2015). The uncertainties in the periods derived for the transit groups a–f are too large to identify them with any of the features from Croll et al. (2015).

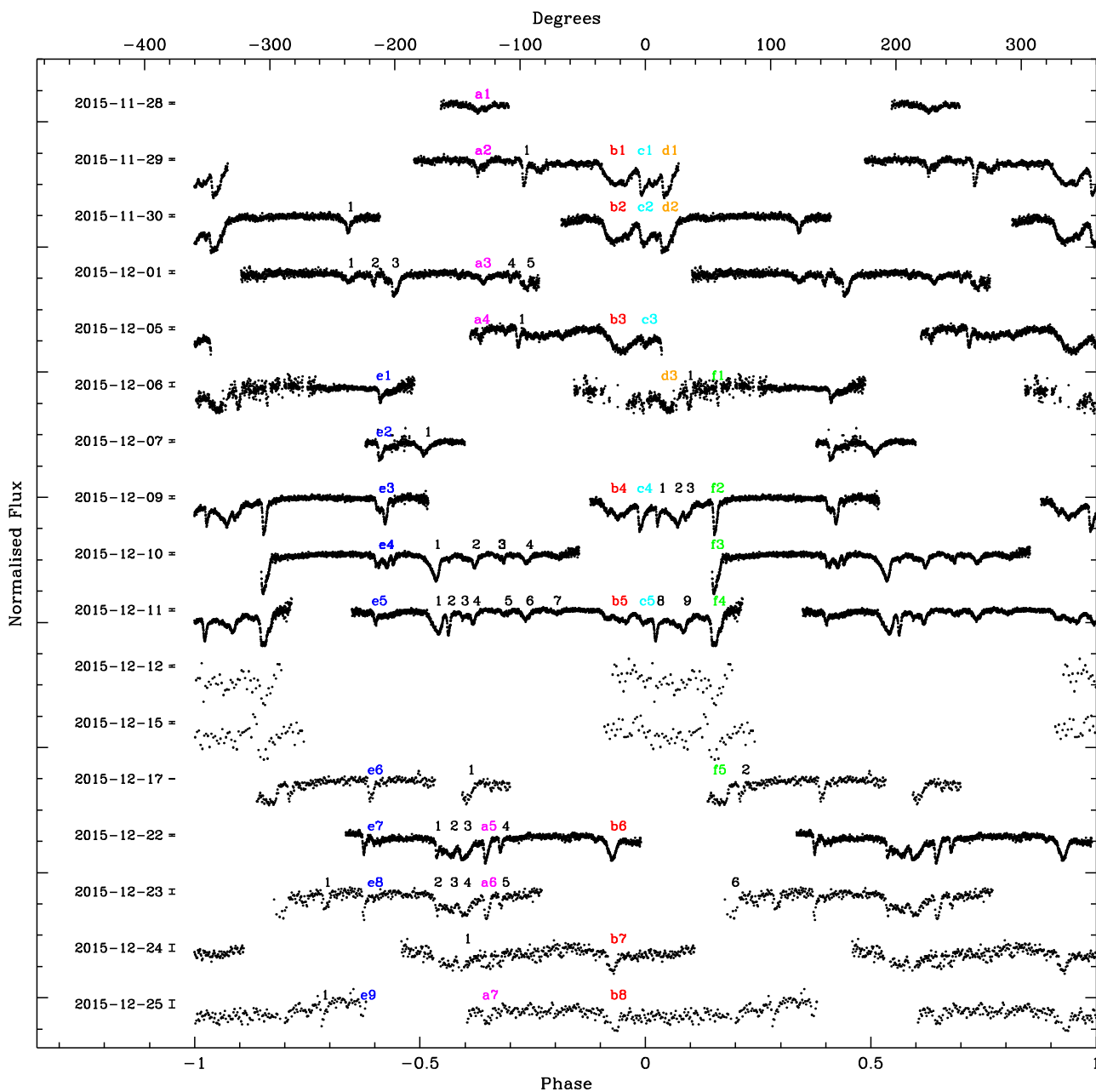


Figure 2. TNT and Warwick 1 m light curves of WD 1145+017, folded on a period of 4.4930 hr, two orbital cycles are shown for clarity. Typical photometric uncertainties are shown on the right to the observing dates. The observations on December 6 and 7 were affected by cirrus, and some poor quality data was removed. Transit events that can be tracked across multiple nights are labeled in color, and were used for a linear ephemeris fit (Table 1).

Table 1

Orbital Periods Derived from a Linear Ephemeris Fit to the Six Groups of Transit Events Identified in Figure 2

Transits	Period (hr)	Uncertainty (hr)
a	4.49337	0.00021
b	4.49252	0.00011
c	4.49257	0.00052
d	4.49355	0.00040
e	4.49110	0.00006
f	4.49513	0.00046
mean	4.4930	0.0013

Note. The phase stability of the transits is shown in Figure 3.

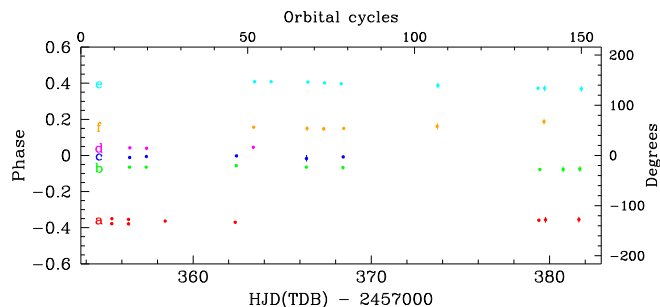


Figure 3. Relative phases of the six transit events that we identified across multiple nights adopting a period of 4.4930 hr. The color coding of the transits is the same as in Figure 2.

The light curves, folded on the mean period derived from the linear ephemeris analysis (Figure 2) clearly show that the structure and evolution of the debris orbiting WD 1145+017 is extremely complex. Many of the transit events show sub-structure that changes from night to night (e.g., e2–e4), other strong features gradually appear (e.g., f2–f5, with possibly a weak pre-cursor, f1), while others intermittently disappear (e.g., the “a” transit is not detected on December 10, 11, 17). While we cannot exclude the presence of transits recurring on different periods, the stability of the relative phases of several groups of transit events suggests the presence of many, co-orbital, debris bodies at WD 1145+017.

4. DISCUSSION

The optical transit events observed by Vanderburg et al. (2015) and Croll et al. (2015) had a sharp ingress and a slow egress, reminiscent to those of the disintegrating planets KIC 12557548b (Rappaport et al. 2012) and KOI 2700b (Rappaport et al. 2014). In all three cases, the long egress was interpreted as a comet-like tail trailing the transiting object (Rappaport et al. 2012; Budaj 2013; Vanderburg et al. 2015).

Most of the transit events in our observations (Figure 2) are fairly symmetric, which is a clear change with respect to the previous observations of WD 1145+017. One of the transits, 2015 December 10#1 and 2015 December 11#1, exhibits a slow ingress and sharp egress, possibly suggesting ejection of dust in the leading direction of the planetesimal. A similar, though much less pronounced, transit shape has been observed in the *K2* light curve of the candidate disintegrating planet K2-22b, where it was modeled with Roche lobe overflow of the planet (Sanchis-Ojeda et al. 2015). The rapid changes seen in the light curve of WD 1145+017, compared to the currently known disintegrating (candidate) planets, KIC 12557548b, KOI 2700b and K2-22b, indicates a much faster evolution of the planetesimals orbiting the white dwarf.

Because of the high time resolution of our data, all individual events are fully resolved, and it is evident that there is a minimum width of the transits, $\simeq 3$ minutes. For comparison with these short transit features, we calculated the eclipse of the white dwarf by opaque spheres. The spheres were assumed to be in circular orbits of period 4.49 hr and to have negligible mass compared to the white dwarf. The mass of the white dwarf was taken to be $0.6 M_{\odot}$ from which its radius ($R_{\text{wd}} = 0.0124 R_{\odot}$) and the orbital semimajor axis ($a = 1.161 R_{\odot}$) follow from the white dwarf mass–radius relation and *Kepler’s* third law, respectively. The white dwarf was assumed to be limb-darkened with a linear limb darkening coefficient of 0.3, leaving the orbital inclination and the radius of the obscuring sphere as the only free parameters. The flux at any given phase was calculated by splitting the visible face of the white dwarf into a regular series of 200 annuli using the Python/C code developed for the eclipsing double white dwarf CSS 41177 (Bours et al. 2014). In this model, the size of the white dwarf largely defines a lower limit to the durations of the transits.

The widths of the observed short-duration transits require the occulting objects to be 2–4 times the size of the white dwarf. Synthetic transit profiles for an inclination of $87^{\circ}.75$ and a transiting object four times bigger than the white dwarf are superimposed on several of the narrow transit events detected in the TNT/ULTRASPEC light curve of WD 1145+017 on 2015 December 11 (scaled for the different transit depths,

being equivalent to different opacities of the debris clouds). Our admittedly simplistic model provides a reasonably good match to the symmetric transit profiles, with no need for a trailing tail used to fit the earlier observations (Croll et al. 2015; Vanderburg et al. 2015). The large physical extent of the material causing the transits (several Earth radii), together with the rapid variability of their shapes and depths, corroborates the conclusion of Vanderburg et al. (2015) that the transits are not caused by solid bodies, but by clouds of gas and dust flowing from significantly smaller objects that remain undetected. The presence of gas along the line of sight was verified by the Keck/HIRES spectra obtained by Xu et al. (2016). The time-averaged extinction throughout the TNT observations is $\tau \simeq 11\%$. Adopting an absorption coefficient of $\kappa(V+B) = 1000 \text{ cm}^2 \text{ g}^{-1}$ in the visual-blue (Ossenkopf et al. 1992) and a uniform dust distribution in a cylindrical sheet of radius a and height $2R_{\text{wd}}$, we estimate $M_{\text{dust}} = 2\pi a \times 2R_{\text{wd}} \tau \kappa^{-1} \simeq 10^{17} \text{ g}$ to explain the observed extinction. This value should be considered as a lower limit, as the vertical extension of the dust is likely larger than the white dwarf. The observed rapid variability of the transit features suggests that this dust mass could be replenished on timescales of days, which would imply a dust production rate of $\sim 10^{11} \text{ g s}^{-1}$, similar to the highest accretion rates onto metal-polluted white dwarfs (Girven et al. 2012). The (presumably rocky) planetesimals may be too small to be detected in ground-based photometry, or alternatively their orbital inclination may be such that they do not transit the white dwarf. In the latter case, the observed transits are likely to be partial, arising from an expanding gas and dust envelope around the solid bodies.

For a typical white dwarf mass of $\simeq 0.6 M_{\odot}$, an orbital period of 4.49 hr is close to the tidal disruption radius of a strengthless rubble-pile with a density of $\simeq 3\text{--}4 \text{ g cm}^{-3}$ (Davidsson 1999; Jura 2003; Veras et al. 2014b). The fact that the planetesimals at WD 1145+017 have been in these orbits for at least $\simeq 550$ days, or $\simeq 3000$ orbital periods, (the *K2* Campaign 1 data was obtained 2014 June to August) suggests that they have low eccentricities: tidal disruption is a strong function of orbital pericentre and almost independent of semimajor axis (Veras et al. 2014b), suggesting that radial incursions due to a nonzero eccentricity would cause disruption on a timescale much shorter than the observed lifetime of the planetesimals. If the parent body had significant internal strength, it could survive within the Roche-radius, allowing for a mild eccentricity of the orbit.

The origin of the planetesimals on close-in, nearly circular orbits at WD 1145+017 remains challenging to explain, particularly because of their unknown size.

If the observed signatures represent fragments of just one large ($R \gtrsim 1000 \text{ km}$) parent body, then a possible scenario for its origin is the following: (1) within the protoplanetary disc, several planets formed at or migrated to a distance of several au, (2) during the giant branch phases of the WD 1145+017 progenitor, the orbits of these planets were pushed outward by a factor of a few, (3) after the star became a white dwarf, the planets underwent a scattering event, causing one planet to achieve a highly eccentric orbit with a pericentre that lay just at the edge of the white dwarf Roche radius, (4) tidal interactions circularized this orbit, while concurrently the close proximity to the white dwarf sheared off portions of the planet and sublimated some of its material. The first three parts of the

above situation are visualized in Figure 1 of Veras & Gänsicke (2015). The fourth part appears viable because of the likely similarity to the tidal circularization process of planets around main sequence stars (see Section 5 of Veras 2016). The disruption, and subsequent accretion of a (minor) planet would result eventually in an extreme metal-pollution of WD 1145+017. While the above sequence appears fine-tuned, several other white dwarfs are known to have accreted at least 10^{24} – 10^{25} g of mainly rocky debris (Girven et al. 2012), equivalent to the masses of Ceres to Pluto. WD 1145+017 has already accreted a minimum of $\simeq 6.6 \times 10^{23}$ g (Xu et al. 2016), which does not account for the unknown mass still in orbit around it.

If, in contrast, the observations are the consequence of one or more asteroid-sized (~ 1 km) bodies on nearly circular orbits, then a similar scenario as outlined before is unlikely to work because the asteroid would induce a tidal bulge on the white dwarf that is too small (e.g., consider a white dwarf-equivalent version of Equations (1)–(2) of Mustill & Villaver 2012) to circularize the orbit. The asteroid further would be too large to be circularized by radiation alone, either through the Yarkovsky effect or Poynting-Robertson drag (Veras et al. 2015a, 2015c). One possibility is that some fraction of the asteroid has sublimated. Although the impulsive perturbation from this process would not change the orbital pericentre (Veras et al. 2015b), the gas generated at the orbital pericentre might drag the asteroid into a circular orbit. Circumstellar gas has been detected at WD 1145+017 (Xu et al. 2016), and gaseous components of debris disks have been identified at several other white dwarfs (Gänsicke et al. 2006, 2008; Melis et al. 2012). However, it is unclear if the amount of gas in these systems is sufficient to significantly contribute to the circularization process. In contrast to comets where out-gassing of volatiles can free copious quantities of gas, most metal-polluted white dwarfs are best explained by the accretion of volatile-depleted asteroids (e.g., Gänsicke et al. 2012; Xu et al. 2014, with possibly a few exceptions, Farihi et al. 2013; Raddi et al. 2015), where gas production via sublimation is less efficient.

In either case, the time over which we can expect to observe the breakup of the planetesimal is highly dependent on just how close it lies to the boundary of the Roche sphere (Veras et al. 2014b), which is non-trivially dependent on the unknown physical properties of the asteroid. Accompanying the tidal fragmentation might be breakup due to rotational fission (Veras et al. 2014a), which is or is not occurring depending on the previous spin rate of the asteroid as it settled into its current orbit. For an older and cooler white dwarf like WD 1145+017, fragmentation due to penetration into the Roche sphere would likely be the dominant breakup mechanism.

5. CONCLUSIONS

High-speed photometry of WD 1145+017 obtained over a period of four weeks reveals frequent transit events with a range of durations, and reaching depths of up to 60%. The shortest events last $\simeq 3$ minutes, and require an obscuring debris cloud that is a few times the size of the white dwarf. Longer transits have significant sub-structure, and often appear to be superpositions of several individual events. Several groups of transits are identified across multiple nights and repeat on periods of 4.491 to 4.495 hr, slightly shorter than the periodicity determined from the *K2* data. The planetary debris

at WD 1145+017 appears to be undergoing a rapid evolution, and continued observations are encouraged to determine how many disintegrating bodies are orbiting this white dwarf, and whether their nearly co-orbital configuration remains stable over longer periods of time. Simultaneous multi-color photometry would provide some insight into the grain size distribution and composition, (e.g., Bochinski et al. 2015; Croll et al. 2015), and possibly into changes of these parameters with time, as the system keeps evolving.

We thank the referee for the very prompt and constructive report. This work has made use of data obtained at the Thai National Observatory on Doi Inthanon, operated by NARIT. The research leading to these results has received funding from the European Research Council under the European Union’s Seventh Framework Programme (FP/2007-2013)/ERC Grant Agreement n. 320964 (WDTracer). A.A. acknowledges the supports of the Thailand Research Fund (grant no. MRG5680152) and the National Research Council of Thailand (grant no. R2559B034). VSD and TRM acknowledge the support of the Royal Society and the Leverhulme Trust for the operation of ULTRASPEC at the TNT. TRM acknowledges support from the Science and Technology Facilities Council (STFC), grant ST/L000733/1.

REFERENCES

- Berg, C., Wegner, G., Foltz, C. B., Chaffee, F. H. J., & Hewett, P. C. 1992, *ApJS*, **78**, 409
- Bochinski, J. J., Haswell, C. A., Marsh, T. R., Dhillon, V. S., & Littlefair, S. P. 2015, *ApJL*, **800**, L21
- Bours, M. C. P., Marsh, T. R., Parsons, S. G., et al. 2014, *MNRAS*, **438**, 3399
- Budaj, J. 2013, *A&A*, **557**, A72
- Cassan, A., Kubas, D., Beaulieu, J.-P., et al. 2012, *Natur*, **481**, 167
- Croll, B., Dalba, P. A., Vanderburg, A., et al. 2015, arXiv:1510.06434
- Davidsson, B. J. R. 1999, *Icar*, **142**, 525
- Debes, J. H., Kilic, M., Faedi, F., et al. 2012, *ApJ*, **754**, 59
- Debes, J. H., & Sigurdsson, S. 2002, *ApJ*, **572**, 556
- Dhillon, V. S., Marsh, T. R., Atkinson, D. C., et al. 2014, *MNRAS*, **444**, 4009
- Farihi, J., Gänsicke, B. T., & Koester, D. 2013, *Sci*, **342**, 218
- Fressin, F., Torres, G., Charbonneau, D., et al. 2013, *ApJ*, **766**, 81
- Friedrich, S., Koester, D., Christlieb, N., Reimers, D., & Wisotzki, L. 2000, *A&A*, **363**, 1040
- Gänsicke, B. T., Koester, D., Farihi, J., et al. 2012, *MNRAS*, **424**, 333
- Gänsicke, B. T., Koester, D., Marsh, T. R., Rebassa-Mansergas, A., & Southworth, J. 2008, *MNRAS*, **391**, L103
- Gänsicke, B. T., Marsh, T. R., Southworth, J., & Rebassa-Mansergas, A. 2006, *Sci*, **314**, 1908
- Girven, J., Brinkworth, C. S., Farihi, J., et al. 2012, *ApJ*, **749**, 154
- Jura, M. 2003, *ApJL*, **584**, L91
- Koester, D., Gänsicke, B. T., & Farihi, J. 2014, *A&A*, **566**, A34
- Manser, C. J., Gänsicke, B. T., Marsh, T. R., et al. 2016, *MNRAS*, **455**, 4467
- Melis, C., Dufour, P., Farihi, J., et al. 2012, *ApJL*, **751**, L4
- Mustill, A. J., & Villaver, E. 2012, *ApJ*, **761**, 121
- Ossenkopf, V., Henning, T., & Mathis, J. S. 1992, *A&A*, **261**, 567
- Pyrzas, S., Gänsicke, B. T., Thorstensen, J. R., et al. 2012, *PASP*, **124**, 204
- Raddi, R., Gänsicke, B. T., Koester, D., et al. 2015, *MNRAS*, **450**, 2083
- Rappaport, S., Barclay, T., DeVore, J., et al. 2014, *ApJ*, **784**, 40
- Rappaport, S., Levine, A., Chiang, E., et al. 2012, *ApJ*, **752**, 1
- Rocchetto, M., Farihi, J., Gänsicke, B. T., & Bergfors, C. 2015, *MNRAS*, **449**, 574
- Sanchis-Ojeda, R., Rappaport, S., Pallé, E., et al. 2015, *ApJ*, **812**, 112
- Vanderburg, A., Johnson, J. A., Rappaport, S., et al. 2015, *Natur*, **526**, 546
- Veras, D. 2016, RSOS, in press (arXiv:1601.05419)
- Veras, D., Eggl, S., & Gänsicke, B. T. 2015a, *MNRAS*, **451**, 2814
- Veras, D., Eggl, S., & Gänsicke, B. T. 2015b, *MNRAS*, **452**, 1945
- Veras, D., & Gänsicke, B. T. 2015, *MNRAS*, **447**, 1049
- Veras, D., Jacobson, S. A., & Gänsicke, B. T. 2014a, *MNRAS*, **445**, 2794
- Veras, D., Leinhardt, Z. M., Bonsor, A., & Gänsicke, B. T. 2014b, *MNRAS*, **445**, 2244

Veras, D., Leinhardt, Z. M., Eggl, S., & Gänsicke, B. T. 2015c, [MNRAS](#), [451](#), [3453](#)
Veras, D., Mustill, A. J., Bonsor, A., & Wyatt, M. C. 2013, [MNRAS](#), [431](#), [1686](#)
Wilson, D. J., Gänsicke, B. T., Koester, D., et al. 2014, [MNRAS](#), [445](#), [1878](#)
Wilson, D. J., Gänsicke, B. T., Koester, D., et al. 2015, [MNRAS](#), [451](#), [3237](#)

Xu, S., & Jura, M. 2014, [ApJL](#), [792](#), [L39](#)
Xu, S., Jura, M., Dufour, P., & Zuckerman, B. 2016, [ApJL](#), [816](#), [L22](#)
Xu, S., Jura, M., Koester, D., Klein, B., & Zuckerman, B. 2014, [ApJ](#), [783](#), [79](#)
Zuckerman, B., Koester, D., Reid, I. N., & Hüensch, M. 2003, [ApJ](#), [596](#), [477](#)